Shipping remains a globally significant source of anthropogenic PN emissions even after 2020 sulfur regulation

Niina Kuittinen[a], Jukka-Pekka Jalkanen[b], Jenni Alanen[a], Leonidas Ntziachristos[a], Hanna Hannuniemi[b], Lasse Johansson[b], Panu Karjalainen[a], Erkka Saukko[a], Mia Isotalo[a], Päivi Aakko-Saksa[c], Kati Lehtoranta[c], Jorma Keskinen[a], Pauli Simonen[a], Sanna Saarikoski[b], Eija Asmi[b], Tuomas Laurila[b], Risto Hillamo[b], Fanni Mylläri[a], Heikki Lihavainen[b,d], Hilkka Timonen[b], Topi Rönkkö[a]*

[a]Aerosol Physics Laboratory, Faculty of Engineering and Natural Sciences, Tampere University, FI-33014, Tampere, Finland

[b]Atmospheric Composition Research, Finnish Meteorological Institute, P.O. Box 503, 00101 Helsinki, Finland
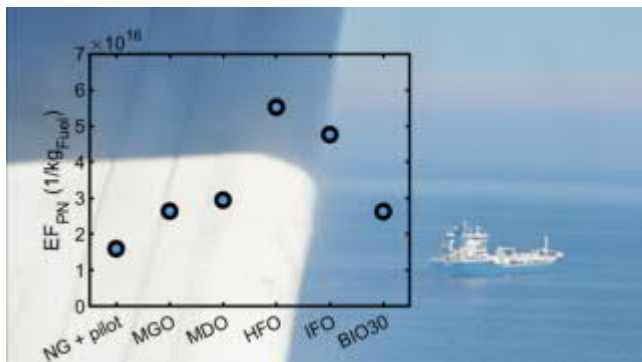
[c]VTT Technical Research Centre of Finland Ltd., P.O. Box 1000, 02044 VTT, Espoo, Finland

[d]Svalbard Integrated Arctic Earth Observing System, P.O. Box 156, 9171 Longyearbyen, Norway

ABSTRACT

Shipping is the main source of anthropogenic particle emissions in large areas of the globe, influencing climate, air quality, and human health in open seas and coast lines. Here we determined, by laboratory and on-board measurements of ship engine exhaust, fuel-specific particle number (PN) emissions for different fuels and desulfurization applied in shipping. The emission factors were compared to ship exhaust plume observations and, furthermore, exploited in the assessment of global PN emissions from shipping, utilizing STEAM ship emission model. Results indicate that most particles in the fresh ship engine exhaust are in ultrafine particle (UFP) size range. Shipping PN emissions are localized especially close to coastal lines but significant emissions exist also on open seas and oceans. The global annual PN produced by marine shipping was 1.2×10^{28} ($\pm 0.34 \times 10^{28}$) particles in 2016, thus being of same magnitude with total anthropogenic PN emissions in continental areas. The reduction potential of PN from shipping strongly depends on the adopted technology mix, and except wide adoption of natural gas or scrubbers, no significant decrease in global PN is expected if heavy fuel oil is mainly replaced by low sulfur residual fuels. The results imply that shipping remains as a significant source of anthropogenic PN emissions that should be considered in future climate and health impact models.

INTRODUCTION

Ambient particles produced by combustion sources contain elevated concentrations of black carbon, heavy metals and semi-volatile organic and inorganic compounds (1). Particulate emissions contribute significantly to climate forcing (2-4), depending on their concentration and properties. Combustion aerosols indirectly affect climate by influencing the formation of clouds and their light scattering properties. This indirect effect has been clearly observed when marine vessels form 'ship tracks', i.e., clouds produced when water condenses on aerosol particles produced by ship engine exhaust, under certain environmental conditions. (5, 6). These ship tracks further affect the total cloud albedo in the area (7, 8). Certain particles may also induce ice nucleation, which has climatic implications especially in pristine environments, like the Arctic (9), or they may change precipitation patterns (10). In order to accurately estimate the climate-forcing impacts of ship emissions, particle number (PN) and size distribution (PSD) of the emitted aerosols are important, further to total particle mass (PM) (11, 12).

Shipping activities also contribute significantly to air-pollution related health effects (2, 7, 13). Because the PN frequently indicates the number of ultrafine particles (below 100 nm in size), it represents also the particles depositing efficiently to the alveolar region of lungs (14), being able to translocate in the body (15), and having large surface area for possible adsorption and transportation of toxic compounds (16, 17, 18, 19, 20) to the human body. UFPs have been linked to various negative health effects and their quantification in the freshly emitted exhaust is needed to further consider exposure related health effects (17, 21).

As one response to the effects of air pollution from shipping, the International Maritime Organization has set a global cap of 0.5% for the fuel sulfur content (FSC) in marine fuels that

took place in the beginning of 2020. This followed the establishment of emission control areas

(ECAs) where FSC has already been limited to 0.1%. Several options are available for ship

owners to meet these new limits. Before 2020, majority of the global fleet burned heavy fuel oil

(HFO) with sulfur content up to 3.5%. Shift to lower sulfur fuels such as intermediate fuel oil

(IFO), marine gasoil (MGO) or marine diesel oil (MDO), conversion of engines to run on

liquefied natural gas (LNG), or use of sulfur scrubbers for exhaust desulfurization are the most

evident options. Although these methods bring exhaust sulfur concentration to levels consistent

with the regulatory requirements, their comparative effects on PN concentrations in freshly

emitted exhaust have not been collectively reported.

Particles originated from ship engines can form during high-temperature, high-pressure

combustion in the diesel engine cylinders or, in principle, they can be formed when precursor

gases nucleate and condensate during the cooling and dilution of the exhaust. At the moment, the

only regulated method for measuring PN from ships considers solid particles larger than 23 nm

in diameter and is applied only for new and large ship engines used in inland waterway vessels

(e.g. 22). However, the aerosol processes in cooling and diluting exhaust may significantly

increase the total PN emitted and affect the size of the particles. Significant fraction of these

particles can be below the above-mentioned 23 nm particle size (23). Thus, to understand the

real-life PN emissions from shipping, also the semi-volatile particles potentially formed during

exhaust cooling should be considered, both in measurements and in modeling studies.

Several studies report PN emission factors (EF$_{PN}$) measured from freshly emitted ship plumes for

a vast number of ships. For example, Lack et al. (24) report average emission factor of 1.0×10^{16}

kg$_{fuel}$$^{-1}$ for 60 ships burning fuel with FSC above 0.5%, and average emission factor of 7.0×10^{15}

kg$_{fuel}$$^{-1}$ for 83 ships burning fuel with FSC below 0.5%. Also, Diesch et al. (25) and Jonsson et al.

(26) report average emission factors of 2.6×10^{16} kg$_{fuel}$$^{-1}$ for 139 ships and 3.2×10^{16} kg$_{fuel}$$^{-1}$ for

92 ships, respectively, all navigating within ECAs applying 1.0% sulfur limit at the time. In

plume studies where the fuel quality is specified, PN emission factors varying between 0.4-4.7 $\times$

10^{16} kg$_{fuel}$$^{-1}$ have been reported for HFO (27, 28, 29, 30, 31), 6.2×10^{16} kg$_{fuel}$$^{-1}$ for IFO (32), and

emission factors between 0.45-4.0 $\times 10^{16}$ kg$_{fuel}$$^{-1}$ distillate fuels (27, 30, 32, 33, 34).

In this study, we investigate experimentally the effects of fuel changes and exhaust scrubbing on

total PN present in freshly emitted ship engine exhaust. We compare these results, i.e., PN

emission factors and PSDs determined in laboratory and on-board by utilizing direct exhaust

sampling, to the PN emission factors and PSDs determined by chasing real atmospheric ship

plumes. Finally, we use the PN emission factors for different technology options in global level

assessment of shipping emitted PN and discuss about the roles of fuel choices and exhaust

cleaning in respect of the development of PN emissions of shipping, especially regarding the

recently adopted global sulfur cap.

MATERIALS AND METHODS

   Engine exhaust experiments. Laboratory experiments were made with a four-cylinder, four-

stroke, medium-speed Wärtsilä Vasa 4R32 LN E ship engine (nominal power 1640 kW, Table S1)

at two load conditions, i.e., at 25% and 75% of maximum load, representing typical maneuvering

operation at port and open-seas cruising operation, respectively. The engine was preconditioned

for 200 h with a Shell Argina XL lubricant oil, used also during actual measurements. The fuels

tested (Table S2) were an HFO, an IFO, and a 30% vol. biofuel mixed with MGO-quality light

fuel oil (BIO30). The FSCs were 2.2%, 0.375%, and below 5 ppm, respectively. Sufficient engine

running time was reserved for fuel changes between the particle measurements to avoid any

residues in the engine. When combined with our previous study (23), the studied fuels cover the majority of fuel types used in shipping activities.

The particle removal efficiency of a sulfur scrubber was determined with two engines on-board a modern cruise ship. Engines' nominal powers were 9.6 MW (Engine A, equipped with selective catalytic reduction (SCR) before the scrubber) and 14.4 MW (Engine B). Both engines were fueled by HFO (denoted as HFO 0.7% S, see Table S2), and used the same scrubber but only one engine was run at a time. The studied engine load conditions were 75% and 40%.

Both in laboratory and on-board experiments the exhaust was sampled from tailpipe (Figure S1) and diluted with a porous tube diluter (PTD) coupled with a residence time tube (35) and then with an ejector diluter, resulting in a total residence time of 2.6 s in the primary dilution system. The combination has previously been shown to mimic real fresh exhaust plume in terms of semi-volatile compounds, PN, and PSD during the first seconds and minutes after the emission (1, 36-38). The primary dilution air was heated to 30°C and the nominal dilution ratios (DR) were 12 for PTD and 8 for ejector. Additional dilution was provided with ejectors (39) and with bridge-type diluters. Actual DRs were monitored with continuous CO_2 measurements. In both campaigns, the PN was measured using an Airmodus A20 condensation particle counter (CPC) with a cut-point at 7 nm. PSDs were measured using scanning mobility particle sizers (SMPS: DMA 3071A and CPC 3775, TSI Inc., size range 10-414 nm; nano-SMPS: DMA 3085 and CPC 3776, TSI Inc., size range 3-64 nm). We observed a clogging tendency in the ejector diluter, which increased slowly the DR of the secondary dilution (total DR of the PTD-residence time tube-ejector setup varied in laboratory campaign from 75 to 370 and in onboard campaign from 123-196). For this reason, real-time DRs were always used in data processing. During on-board campaign the dilution air temperature varied between 33-39 °C. PN emission factors (Table S3) were calculated using CPC

concentrations together with engine power, fuel consumption and exhaust mass flow calculated based on the carbon balance method. Density for the wet exhaust gas was approximated according to the ISO 8178.

Real ship plume experiments. The real-world experiments were performed with research aircrafts in the Gulf of Finland in the Baltic Sea (Figure S3). Three sets of flights were carried out during the spring 2013 (with Reims-Cessna FR172F airplane in January 25, February 25-26, and March 7-8; with Eurocopter EC135 helicopter in March 28, April 3, and April 9; with Aalto University's Short Skyvan SC-7 research airplane in May 16, 17, 21, and 24). In each set, the research aircraft located target ships and flew along their plumes as close as possible to their funnel exhaust. Background levels for PN and CO_2 (Figures S6-S9) were measured when neither visual perceptions of ships were made nor peaks in CO_2 or particle number were observed. EF_{PN} were calculated for time periods of simultaneously elevated PN and CO_2 concentrations, and background concentrations were deducted. Table S4 shows list of the chased ships, their PN emission factors, and the fuel sulfur contents verified by the ship operators.

In chasing experiments, the Skyvan aircraft was equipped with a BMI Isokinetic Inlet System (Model 1200, Brechtel Manufacturing Inc., USA). With the two lighter aircrafts, a simple air intake tube with an outer diameter of 10 mm and a length of 2 m was applied, designed for sampling the ambient air to on-board instrumentation with minimum losses. The CO_2 was measured with a Picarro G1301-m (Picarro Inc.; time resolution 1 s, accuracy 0.05 ppm, response time ~2s) (40) analyzer. Particles were measured with CPCs (TSI model 3776 with 3 nm cut-point, first two sets of flights; TSI model 3010 with 10 nm cut-point, the last set of flights), and with an Engine Exhaust Particle Sizer (41) (EEPS, TSI Inc., size range 5.6-560 nm with the default inversion algorithm, the last set of flights). The aircraft position and speed data were recorded with GPS. The emission

rate for PN was calculated using the data provided by the CPC and the CO_2 analyzer, according to equation 1 in Pirjola et al. (42). Time integrals of instrument signal peaks were used because of slightly differing response times of the instruments. From the emission rate, EF_{PN} was calculated again following the method (equation 2b) described by Pirjola et al. (42) and applying the emission factor 3.107 kg/kg_{fuel} (43) for CO_2. The method to calculate the atmospheric age of the sampled exhaust plume is described in SI.

Evaluating global PN emissions from shipping. The global fuel consumption for the marine shipping in 2016 was calculated with the Ship Traffic Emission Assessment Model (STEAM, version 3) (44-47). Global Automatic Identification System (AIS) data from both terrestrial and satellite networks were obtained from Orbcomm. For each cruising vessel, the technical description was obtained from IHS Fairplay and the fuel use and emissions were modelled by applying water resistance calculations on the speeds indicated by the AIS data. STEAM considers the fuel consumption and quality both in auxiliary and main engines of the vessels. In total, the model run included 248,000 ships, out of which 59,000 were registered by the IMO, and 2.9 billion AIS messages. Smart routing (47) was applied to mitigate the impact of incomplete AIS coverage in some areas, mostly in South-East Asia. The fuel consumption from inland waterways and small boats was not included. For example, in the Baltic Sea, annual AIS recordings cover 8,000-8,500 large vessels, but the number of smaller boats exceeds 250,000. However, in the Baltic Sea region their contribution to total fuel consumption has been found to be less than 1.5%. (48).

Fuel type per vessel was designated according to engine characteristics and sulfur limitations in specific locations (i.e. ECAs). Possible regional variations in the characteristics of a certain fuel type were not considered and would be subject to another study. Changes in specific fuel oil consumption (SFOC) of marine engines were considered assuming a parabolic dependency of

SFOC as function of engine load (45). In 2016, scrubber installations were included in STEAM and accounted for 0.2% of the fleet. Additional power consumption of 3% was accounted for vessels applying open-loop scrubbers (see SI for details). With these assumptions, the fuel consumption of the global fleet in 2016 was estimated to Table S5. Uncertainty of 15% is inferred based on comparisons of annual fuel consumptions of ships included in the EU MRV reporting scheme (only available 2018 onwards).

In the base estimate for 2020, total energy consumption of 1.16×10^{13} MJ derived from STEAM model run was assumed (2), indicating 8.6% increase when compared to 2016. Because data on the adoption of different marine fuel qualities in 2020 was not available, contributions of different fuels to total fuel consumption in 2020 were assumed based on industry reports. In this estimate, shift from HFO to residuals with lower sulfur content as well as introduction of scrubbers and conservative increases in LNG (from 2% in 2016 to 3% in 2020, of total fuel use (49, 50)) and biofuel consumption (0.3% of total fuel use (49)) were included. Estimates for the share of scrubber installations in 2020 range between 4-14 % (49, 50); due to the limited dock capacity for scrubber installations, the low estimate of 4% was chosen for the base estimate of 2020. MGO and MDO are assumed to be used only in ECAs, and thus, their relative contributions to global marine fuel consumption would stay constant. In our estimate, we assume that all the remaining fuel usage, which can no longer be covered by HFO, will be replaced with IFO. After this, exact fuel consumptions for each fuel type in were calculated to match the energy need of 1.16×10^{13} MJ, considering different heating value of each fuel type (Table S6). STEAM applies energy densities of 49.7 MJ/kg, 42.70 MJ/kg, 42.70 MJ/kg, 40.25 MJ/kg for LNG, MGO, MDO, HFO, respectively (51). For IFO and BIO30 energy densities from fuel analyses (Table S2) were applied.

The availability of low-sulfur residuals may still be developing in 2020, leading to increased use of distillates with 0.10-0.50% sulfur (50). For this reason, we performed hypothetical calculations studying cases where MDO, MGO, LNG, BIO30 or HFO with scrubber would replace HFO in whole (Figure S10, Table S6). In these calculations, equivalent power output to IFO fuel consumption was covered by the other fuel options being studied, and emitted PN was calculated accordingly, applying kWh-based emission factors. For the 2020 calculations, we used EF_{PN} for IFO to represent the emerging hybrid residual fuels with residual content but sulfur levels below 0.5%. The EF_{PN} for IFO (Figure1) were of similar magnitude with ones reported for low sulfur HFO ($3-12 \times 10^{15}$ kWh^{-1}) (52). EF_{PN} for BIO30 represents the use of biofuels in blends with petroleum derived fuels.

The fuel-based EF_{PN} showed 8-50% higher values at low load conditions. To consider this, a weighted average of low and high load values was applied in STEAM. Adapting the ISO 8178 E3 test cycle, it was assumed that low loads account 30% and high loads 70% of typical ship engine operation. In 2016 run, the effect of scrubber on EF_{PN} was omitted, but for 2020 the scrubber reduction efficiency determined from on-board measurements was accounted for (see SI). Unlike the applied test engine, 2% of the fleet were found to apply common-rail injection systems but this influence on global emissions was estimated to be small.

RESULTS AND DISCUSSION

Test-bench and on-board measurements of ship engine exhaust

The PSDs measured from the exhaust of a test-bench marine engine are presented in Figures 1A and B, together with the PSDs measured with the same engine with NG, MGO and MDO fuels by Alanen et al. (23), shown separately for cruising conditions and maneuvering conditions. In

general, the PSDs exhibited similar shapes for nearly all the studied fuels and conditions; the majority of the particles were in the UFP size range (<100 nm) and in most of the cases nucleation mode particles dominated the distributions. Overall, the combustion of IFO and HFO produced largest particles, i.e., the geometric mean diameters (GMD) of PSDs were around 38-51 nm. Yet, in the case of the HFO at maneuvering load, two dominant particle modes appeared with GMDs around 33nm and 68nm. Smallest particles were emitted when the engine was run with the NG, and the distillate fuel qualities together with the BIO30 blend led to relatively similar GMDs of 23-37 nm. In all cases, the lower load produced larger particles, possibly due to higher soot formation or higher emissions of unburned hydrocarbons that could condensate to particle phase during exhaust dilution and cooling (e.g. 53).

The PN emission factors (Figure 1C) of the test-bench engine varied between 1.4×10^{16} kg_{fuel}^{-1} for NG and 5.4×10^{16} kg_{fuel}^{-1} for HFO during cruising load and between 2.1×10^{16} kg_{fuel}^{-1} for NG and 5.8×10^{16} kg_{fuel}^{-1} for HFO during maneuvering conditions. PN emission factor for IFO during maneuvering, 5.7×10^{16} kg_{fuel}^{-1}, resembled the one for HFO, while during cruising conditions the EF_{PN} was reduced, being 4.4×10^{16} kg_{fuel}^{-1}. MGO, MDO, and BIO30 produced relatively similar PN emissions, EF_{PN} varying between 2.3-2.8$\times10^{16}$ kg_{fuel}^{-1} during cruising and 3.2-3.4 $\times10^{16}$ kg_{fuel}^{-1} during maneuvering load. Thus, results indicate that, compared to HFO, lighter liquid and gaseous fuels decrease PN emissions of marine engines. However, this is not as significant as one would expect from corresponding impacts of fuel changes on emitted particulate mass. For example, Sofiev et al. (2) found a more than threefold decrease in PM when shifting from HFO to MDO, while the corresponding reduction in PN, observed in this study, was less than two-fold. As a phenomenon, the disproportional decrease in PN compared to PM can be explained by an overall shift of exhaust particles to smaller particle sizes (see Figure 1A and 1B). This may

reflect an overall lower availability of exhaust vapors with propensity to condense in the case of lighter fuels (1, 54, 55).
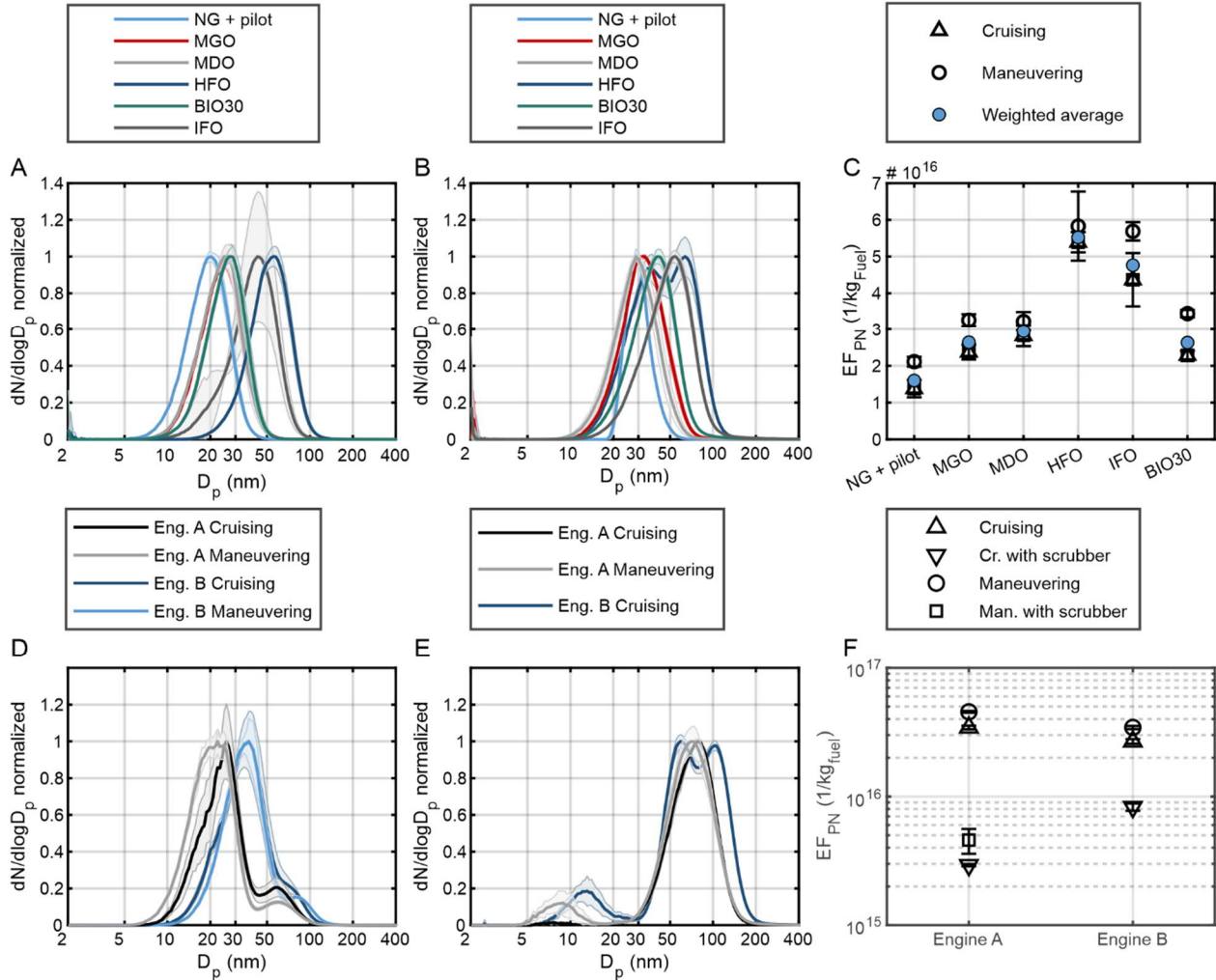
Figure 1. Effects of fuel on particle number size distributions of exhaust from marine engine at engine load representing cruising conditions (A) and maneuvering conditions (B). Normalized mean particle size distributions (PSD) are shown, shaded areas denote one standard deviation. (C) PN emission factors (± standard deviation), calculated from CPC data at cruising and maneuvering conditions and weighted average calculated corresponding to 70% and 30%

contributions from cruising and maneuvering conditions, respectively. Regarding NG+pilot, MGO and MDO fuels, see Alanen et al. (23) Normalized mean particle number size distributions measured on-board for engines A and B in maneuvering and cruising conditions before (D) and after scrubber (E) as well as corresponding particle number emissions factors (F). Engines A and B were fueled with HFO with sulfur content of 0.7%. Engine A is a main engine equipped with SCR, Engine B was not equipped with the SCR. For engine B, EF_{PN} measured after the scrubber is missing at maneuvering load.

Figure 1 also shows PSDs from on-board measurements of marine engine exhaust before (Figure 1D) and after (Figure 1E) the exhaust passed through an open-loop scrubber. Here, the PSDs measured before scrubber showed similar particle size range as in test-bench measurements so that the UFPs clearly dominated the PSDs. However, with both the engines the PSDs were more clearly bimodal with modes between 20 and 40 nm and between 30 and 100 nm. It should be noted that the engines measured on-board had common-rail injection and burned HFO with lower sulfur content which may explain smaller particle size when the engine out exhaust PSDs are compared to laboratory measurements.

The scrubber efficiently removed particles from exhaust, especially in the particle size range below 50nm, and changed the exhaust PSDs; when measured after the scrubber, PSDs show clearly reduced ratio of nucleation mode particles in comparison to larger accumulation mode particles and, in the case of engine B, two particle modes were observed in particle sizes larger than 50 nm. The effect of scrubber was clearly seen in emission factors; while EF_{PN} before scrubber were 2.5-4.2 $\times 10^{16}$ kg_{fuel}^{-1}, after the scrubber they were 2.7-7.7 $\times10^{15}$ kg_{fuel}^{-1} (Figure 1F). Thus, the scrubber significantly reduced the PN emissions, on average by 84% (standard deviation $\pm$ 12%), which is similar to the removal efficiencies found by Fridell & Salo (56)

(92%). The changes in PSDs suggest that the reduction in PN is mainly attributed to nucleation mode particles usually containing volatile species. This is supported by previous studies (22, 57) which do not report clear reduction over scrubber when considering only non-volatile PN.

Particles in atmospheric exhaust plumes from ships
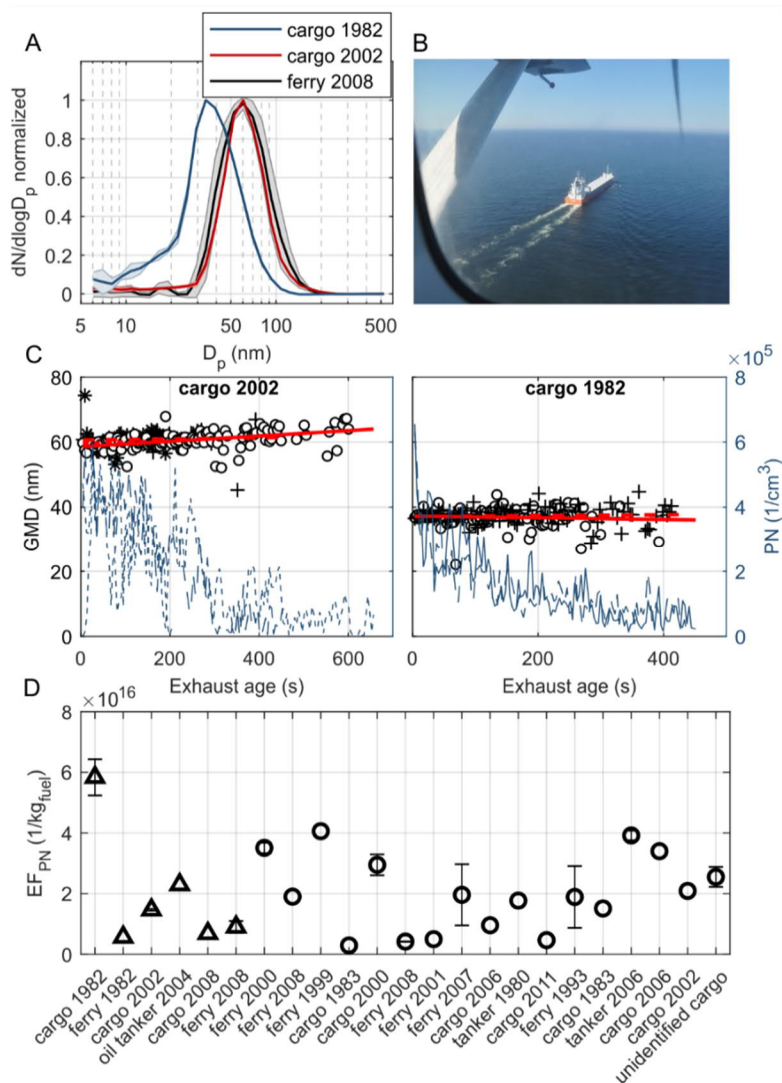
Figure 2. Marine exhaust plume experiment conducted by aircrafts. A. Normalized exhaust plume PSDs as a mean over in-plume flights, shown for three individual ships. The shaded areas denote one standard deviation of measurement points. All 6 ships are shown in Figure S2. B.

View from the research aircraft during approaching a vessel. C. An example of the evolution of geometric mean diameter of exhaust particles (left y-axis) and PN concentration (right y-axis) over in-plume flights, shown as a function of exhaust plume age for two cargo type ships. Varying symbols correspond to separate approaches. PN concentrations are shown in logarithmic scale in Figure S5. D. PN emission factors for 23 vessels. Triangles denote cases when CPC cut-point was 10 nm and circles cases when CPC with a cut-point of 3 nm was applied. Error bars denote one standard deviation of results when the ship was chased at least three times.

Test-bench and on-board measurements of exhaust PN and PSD showed above that the exhaust aerosol from ship engine are affected by fuel, engine load and exhaust treatment by scrubber. This means that, in principle, no exact correspondence is easily found if the details of results above are compared with real exhaust plumes from marine vessels. However, the more general features of sampled exhaust, such as the role of UFPs in PN and the form of PSDs are important to compare with real exhaust, especially because the test-bench and on-board measurements were made for fresh exhaust particles, potentially significantly affected by gas-to-particle processes during exhaust dilution and cooling. To do that, research aircrafts with aerosol instrumentation were used to measure exhaust plume PN (23 vessels) and PSD (6 vessels) of vessels operating in the Baltic Sea (Figure 2). In exhaust plume PSDs, majority of the particles was in a mode with peak diameter varying from 33 to 60 nm, depending on the vessel and, presumably, operation conditions (Figure 2A). In some cases, particles were found also in smaller particle sizes, even down to 10 nm, but they represented minority of the total PN. Overall, the PSDs had relatively similar shapes to those obtained from the test-bench measurements. However, none of the chased ships was applying a scrubber and thus, direct

comparison cannot be made with the exhaust PSD measured on-board after the exhaust treatment with scrubber.

The measured PN concentrations and PSDs were evaluated with respect to time after emission by considering aircraft and vessel cruising speeds as well as wind speed and direction (Figure 2C). We observed that, importantly, the mean diameter of the particles only marginally changed over several minutes after emission (Figure 2C, Figure S5), suggesting that besides dilution seen to gradually decrease the particle concentrations of plumes, no other aerosol dynamics were significant in the measured time scales. For example, particle evaporation would have led to shrinkage, and condensation or coagulation to an increasing mean particle size. Murphy *et al.* (30) also report marginal ship plume PSD changes during the first 24 minutes after atmospheric emission, and unimodal marine exhaust plume PSDs are typically observed for cruising ships, following atmospheric dilution (33, 43, 25). A mode below 13 nm that disappears within 4 minutes after emission, observed by Lack *et al.* (24), was not detected in our study. In general, the results suggest that particles with typical size distributions (see Figure 2A) in the plume of marine vessel exhaust have relatively high atmospheric residence times and, on the other hand, indicate that the results for fresh exhaust aerosol obtained from test-bench and on-board measurements represent real atmospheric exhaust. This can be stated also when the PN emission factors are compared; the EF_{PN} measured on-board and in the test-bench are of same magnitude with EF_{PN} of $0.29\text{-}5.8 \times 10^{16}$ kg_{fuel}^{-1} (Figure 2D) measured during approaches over the plumes of all 23 vessels operating on relatively low-sulfur (<1%) heavy or intermediate fuel oils.

Table 1. PN emission factors for plume, laboratory and on-board measurements conducted in this study, as well as comparison to previously reported plume studies. Studies of ship engine exhaust emissions applying dilution systems which mimic PN in freshly emitted exhaust are

scarce, and for this reason, mainly studies reporting PN from ship plume chase experiments are included.

Fuel	Study	EF_{PN} $(1/kg_{fuel})$	Number of ships	FSC (%)
HFO	Murphy et al. (30)	1.3×10^{16}	1	n/a
	Chen et al. (6)	$4.6 - 4.7 \times 10^{16}$	2	1.9-2.2
	Hobbs et al. (27)	$4.0 \times 10^{15} - 2.2 \times 10^{16}$	5	n/a
	Lack et al. (31)	1.0×10^{16}	1	3.15
	Petzold et al. (29)	1.36×10^{16}	1	2.45
	This study, plume chase	$4.7 \times 10^{15} - 5.8 \times 10^{16}$	11	0.5-1.0
	This study, test-engine	$5.4 - 5.8 \times 10^{16}$	-	2.2
	This study, on-board	$2.5 - 4.2 \times 10^{16}$	-	0.65
IFO	Sinha et al. (32)	6.2×10^{16}	1	2.4
	This study, plume chase	4.2×10^{15}	1	0.87
	This study, test-engine	$4.4 - 5.7 \times 10^{16}$	-	0.375
Distillate	Sinha et al. (32)	4.0×10^{16}	1	0.1
	Hobbs et al. (27)	1.3×10^{16}	1	n/a
	Cappa et al. (33)	2.3×10^{16}	1	0.1
	Aliabadi et al. (34)	$4.5 \times 10^{15} - 2.4 \times 10^{16}$	1	1.5
	Lack et al. (24)	1.4×10^{16}	1	0.07

	This study, test-engine	$2.4 - 3.3 \times 10^{16}$	-	0.0006
	This study, test-engine	$2.8 - 3.2 \times 10^{16}$	-	0.082
NG	This study, test-engine	$1.4 - 2.1 \times 10^{16}$	-	< 0.001
n/a	Lack et al. (24)	2.0×10^{16}	60	>0.5
	Lack et al. (24)	1.0×10^{16}	83	<0.5
	Jonsson et al. (26)	3.2×10^{16}	92	<1
	Diesch et al. (25)	2.6×10^{16}	139	0.38
	Alföldy et al. (62)	1.7×10^{16}	165	<1.5
	This study, plume chase	$2.9 \times 10^{15} - 3.9 \times 10^{16}$	11	n/a

Table 1 compares the values of EF_{PN} measured for engine out exhaust with values reported from other studies that have applied CPC to measure PN emission factors for freshly emitted particles. It can be seen that the EF_{PN} values from this study, obtained by sampling the exhaust directly from tailpipe, are in same range with values reported in previous studies for real atmospheric exhaust plumes. On the other hand, a clear trend between fuel quality and EF_{PN} cannot be derived from the previous studies, partly due to the limited availability of results for IFO and NG. It is also possible that in plume studies the effects of fuels on EF_{PN} are masked by the effects of differences in engine operation, engine characteristics, lubricant oil specifications, as well as atmospheric conditions.
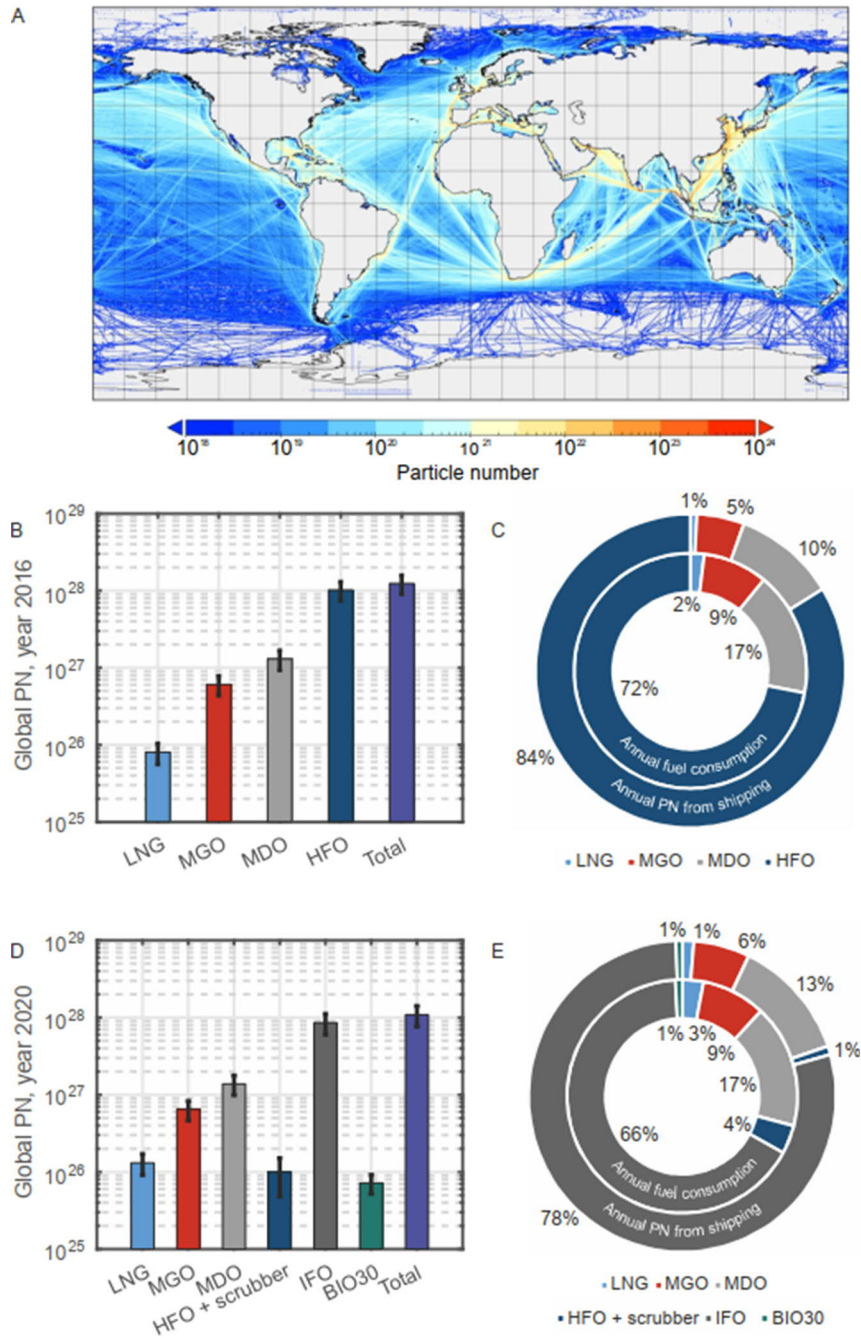
Figure 3. Results for the global PN from shipping in 2016 and scenario in 2020 A. Global distribution of PN emission from ships in 2016. Main shipping lanes between Asia and Europe are clearly visible and high PN values can be found in areas along the route. Color scale denotes total annual particle number emission in a grid cell of 0.1° × 0.1°. B. Annual PN emitted from ship

traffic in 2016 by fuel type. Error bars denote combined uncertainty derived from STEAM output and variation in PN measurement. C. Distribution of annual marine fuel consumption (inner circle) and corresponding PN (outer circle) from different marine fuels on base year 2016. D. Annual PN emitted from ship traffic in 2020 by fuel type according to the base scenario. E. Distribution of annual marine fuel consumption and corresponding PN from different marine fuels in 2020 according to the base scenario.

Estimating global PN from shipping

Although many comprehensive global emission inventories for shipping exist (e.g. 2, 58, 59, 13), they have not considered PN emissions based on global fuel consumption and fuel specific emission factors. However, shipping is a significant PN source globally; e.g. in a study applying a global climate-chemistry model (42), the relative contribution of shipping to global atmospheric PN in 2000 and scenarios for 2030 was estimated to 1-5% globally and up to 9-28% in the North Pacific Ocean. Here we estimated the PN emissions originating from global shipping by applying fuel specific emission factors in STEAM emission model that was run for base year 2016. The IMO sulfur cap adopted in the beginning of 2020 will likely cause use of new fuel types in marine traffic. In order to provide comparison between different fuel qualities and estimate the effect of the 2020 regulation, the weighted EF_{PN} values obtained in experiments of this study were applied. It should be noted that improving the modelling accuracy in the future would benefit from further datasets reporting EFs from freshly emitted PN for different marine fuel options.

Figure 3A shows the global distribution of PN emitted from ship traffic in 2016. It displays elevated PN emission levels on the main oceanic shipping lanes but, importantly, also near

densely populated port cities. From the global PN emission, about 27% were emitted by ships in the South-East Asia (between 12.4°S - 31.3°N and 88.5°E – 153°E). The total number of exhaust particles produced from ship traffic (Figure 3B) was estimated to be 1.22×10^{28} ($\pm0.34\times10^{28}$) annually, being of same order of magnitude as previous estimate for total continental anthropogenic PN emissions of $1.3\text{-}1.5\times10^{28}$ (years 2020 and 2010) (60). Earlier, total value for annual global PN from shipping has been estimated at $0.60\text{-}0.84\times10^{28}$ applying total marine fuel consumption in 1993 (32) and at 0.71×10^{28} applying total fuel consumption in 2009 (26). It should be noted that the total fuel consumption was in 2016 3.2% lower than in 2015 (47), while the total transport work increased by 3.1% and total travel distances by 1% in the same period. The faster growth of transport work than distance indicates that the shift towards larger, more efficient, ships continues. The relative contribution of fuels remained similar to 2015, since no new environmental regulations or control areas were introduced in 2016.

In 2016, the contributions of HFO, MDO, MGO, and LNG on total particle number were 84%, 10%, 5%, and 1%, respectively (Figure 3B). The projection of marine fuel usage in 2020 (Figure 3D) calculated by assuming a net increase of energy demand from shipping activities by 8.6 % (2), introduction of biofuels, moderate increase in the LNG share and scrubber installations, and a shift to residual fuels with sulfur content below 0.5%, indicates that new sulfur regulation is not expected to significantly reduce the PN emitted from ships. When considering the marine fuel usage in 2020 and applying the emission factors presented in this study, total annual PN seems to decrease by only 11% to 1.09×10^{28} ($\pm0.33\times10^{28}$) (Figure 3D) compared to year 2016. This is within the uncertainty of our estimates, suggesting that the effect of the fuel sulfur cap introduction on PN should be considered marginal.

Considering hypothetical calculations where HFO would be replaced in total by either MDO or LNG (Figure S10), instead of intermediate fuel oil (IFO) which still contains residual fuel, the PN reductions in 2020 would be 39% or 61%, respectively. Retaining HFO use and equipping vessels with sulfur scrubbers could lead to even higher reduction of 67% (Figure S10). The calculations in 2020 do not consider the additional power requirement from scrubbers; if accounted for, the reduction of 67% would decrease by 0.4 %-unit. However, feasibility of such wide adoption of either LNG or scrubbers by 2020 is highly unlikely due to limited infrastructure and dock capacity. Thus, after the global sulfur cap in 2020, the PN emission from marine traffic is not expected to significantly decrease, unless distillate fuels, LNG, or emission abatement strategies effective in reducing PN are adapted globally. In case of such adoption, effects on other airborne emissions as well as possible disposals to seawater should be considered holistically. Also, the fuel change may reduce particle toxicity (61) and modelling of consequent health implications, which might not be straight-forward, would merit future study.

Our study implies that shipping remains as a significant source of anthropogenic PN emissions that should be accounted for in future climate modelling and consideration of health impacts. Recent studies have presented exposure models to ultrafine PN (62-65), and the results from this study may help incorporate PN emissions from shipping in exposure models as well as climate models applying direct PN emission inventories (60, 62). The importance of PN emissions from shipping is emphasized by the trend in continental emissions that are dominated by on-road vehicles (60); for these, exhaust particle filters, leading to a decrease of primary PN by orders of magnitude, are becoming mandatory. Therefore, the relative contribution of ship emissions may become higher in the future.

In this study, we focused on particle number emission in fresh exhaust of marine engines. In addition to particles present in the hot exhaust, fresh exhaust contains nucleated particles and PM condensed during the cooling and dilution process (Figure 2C) of the exhaust. Thus, fresh exhaust PN represents best the direct particle emission from the engine to the surrounding atmosphere. After emission, further changes in PN are likely due to agglomeration as well as chemical aging of the exhaust compounds in the atmosphere. This phenomenon, i.e., secondary aerosol formation from emitted compounds, is out of the scope of this study, but its importance is obvious and should be assessed in further studies.

AUTHOR INFORMATION

Corresponding Author

* corresponding author: Topi Rönkkö, Aerosol Physics Laboratory, Faculty of Engineering and Natural Sciences, Tampere University, P.O. Box 692, FI-33014 Tampere University, Finland, topi.ronkko@tuni.fi

Author Contributions

E. S., S. S., E. A., T. L., H. L., R. H. and T. R. designed and conducted the ship chase measurements. N. K., P. K., H. T., P. A.-S., F. M., P. S. and T. R. designed and conducted the first phase of laboratory measurements. N. K., J. A., L. N., P. K., H. T., M. I., K. L., J. K., P. S., T. R. designed and conducted the second laboratory measurements. N. K., P. K., H. T., P. A.-S., and T. R. designed and conducted the on-board measurements. N. K. J. A., E. S., and M. I. conducted data analyses and N. K., J. A., L. N., P. K., H. T., E. S., M. I., P. A.-S., K. L., J. K., and T. R. participated in interpretation of the measurement data. N. K., J.-P. J., H. H., L. J., L. N., and T. R. designed and conducted the global modelling and scenario calculations. N. K., J. A., J.-P. J., L.

N., H. H., and T. R. wrote the manuscript; all authors commented on the manuscript. J.-P. J., H. T., P. A.-S., J. K., H. L., and T. R. made research plans and provided the working environment and financial support.

ASSOCIATED CONTENT

Supporting Information available

Applying CPCs with different cut-points; calculation method for plume age; inclusion of

scrubber installations in STEAM model; instrument setup in laboratory and on-board

measurements; PSDs from chased ships; flight route during chase measurements; logarithmic

particle number concentration as function of plume age; analyzed PN and CPC peaks and

backgrounds during plume measurements; hypothetical calculations on wide adaptation of

different technologies on global PN; details of laboratory engine; details of studied fuels; PN

emission factors obtained from laboratory and on-board measurements; PN emission factors

obtained from plume measurements; global marine fuel consumptions in 2016 obtained from

STEAM and comparison to previous years; global marine fuel consumptions used in calculations

for year 2020. This information is available free of charge via the Internet at http://pubs.acs.org.

REFERENCES

1. Ntziachristos, L., Saukko, E., Lehtoranta, K., Rönkkö, T., Timonen, H., Simonen, P., Karjalainen, P., Keskinen, J. Particle emissions characterization from a medium-speed marine diesel engine with two fuels at different sampling conditions. *Fuel* **186**, 456–465 (2016).

2. Sofiev, M., Winebrake, J. J., Johansson, L., Carr, E. W., Prank, M., Soares, J., Vira, J., Kouznetsov, R., Jalkanen, J., Corbett, J. J. Cleaner fuels for ships provide public health benefits with climate tradeoffs. *Nat. Commun.* **9**, 406 (2018).

3. Tronstad Lund, M., Eyring, V., Fuglestvedt, J., Hendricks, J., Lauer, A., Lee, D., Righi, M. Global-mean temperature change from shipping toward 2050: Improved representation of the indirect aerosol effect in simple climate models. *Environ. Sci. Technol.* **46**, 8868–8877 (2012).

4. Eyring, V., Isaksen, I. S. ., Berntsen, T., Collins, W. J., Corbett, J. J., Endresen, O., Grainger, R. G., Moldanova, J., Schlager, H., Stevensoni, D. S. Transport impacts on atmosphere and climate: Shipping. *Atmos. Environ.* **44**, 4648–4677 (2010).

5. Hudson, J. G., Garrett, T. J., Hobbs, P. V., Strader, S. R., Xie, Y., Yum, S. S. . Cloud Condensation Nuclei and Ship Tracks. *J. Atmos. Sci.* **57**, 2696–2706 (2000).

6. Hudson, J. G., Garrett, T. J., Hobbs, P. V., Strader, S. R., Xie, Y., Yum, S. S. Occurrence of lower cloud albedo in ship tracks. *Atmos. Chem. Phys.* **12**, 8223–8235 (2012).

7. J. J. Winebrake, J. J. Corbett, E. H. Green, A. Lauer, V. Eyring. Mitigating the Health Impacts of Pollution from Oceangoing Shipping : An Assessment of Low-Sulfur Fuel Mandates. *Environ. Sci. Technol.* **43**, 4776–4782 (2009).

8. A. Devasthale, O. Krüger, H. Graßl. Impact of ship emissions on cloud properties over coastal areas. *Geophys. Res. Lett.* **33**, 2–5 (2006).

9. Thomson, E. S., Weber, D., Bingemer, H. G., Tuomi, J., Ebert, M., Pettersson, J. B. C. Intensification of ice nucleation observed in ocean ship emissions. *Sci. Rep.* **8**, 1–9 (2018).

10. J. Fan, D. Rosenfeld, Y. Zhang, S. E. Giangrande, Z. Li, L. A. Machado, S. T. Martin, Y. Yang, J. Wang, P. Artaxo, H. M. J. Barbosa, R. C. Braga, J. M. Comstock, Z. Feng, W. Gao, H. B. Gomes, F. Mei, C. Pöhlker, M. L. Pöhlker, U. Pöschl, R. A. F. Souza. Substantial convection and precipitation enhancements by ultrafine aerosol particles. *Science*, **359**(6374), 411-418 (2008).

11. T. Takemura, T. Nozawa, S. Emori, T. Y. Nakajima, T. Nakajima. Simulation of climate response to aerosol direct and indirect effects with aerosol transport-radiation model. *J. Geophys. Res.* **110**, D02202 (2005).

12. Dusek, U., Frank, G. P., Hildebrandt, L., Curtius, J., Schneider, J., Walter, S., Chand, D., Drewnick, F., Hings, S., Jung, D., Borrmann, S., Andreae, M. O. Size Matters More Than Chemistry for Cloud-Nucleating Ability of Aerosol Particles. *Science* **312**, 1375–1378 (2006).

13. Corbett, J. J., Winebrake, J. J., Green, E. H., Kasibhatla, P., Eyring, V., Lauer, A. Mortality from ship emissions: A global assessment. *Environ. Sci. Technol.* **41**, 8512–8518 (2007).

14. ICRP. Human Respiratory Tract Model for Radiological Protection. ICRP Publication 66. Ann. ICRP **24** (1-3). (1994).

15. Oberdörster, G., Oberdörster, E., Oberdörster, J. Nanotoxicology: An emerging discipline evolving from studies of ultrafine particles. Environmental Health Perspectives, 113(7), 823–839. (2005).

16. Eichler, P., Müller, M., Rohmann, C., Stengel, B., Orasche, J., Zimmermann, R., Wisthaler, A. Lubricating Oil as a Major Constituent of Ship Exhaust Particles. *Environmental Science & Technology Letters,* **4**, 54–58 (2017).

17. Schraufnagel, D. E. The health effects of ultrafine particles. Experimental and Molecular Medicine, **52**(3), 311–317. (2020).

18. Xia, T., Korge, P., Weiss, J. N., Li, N., Venkatesen, M. I., Sioutas, C., Nel, A. Quinones and aromatic chemical compounds in particulate matter induce mitochondrial dysfunction: Implications for ultrafine particle toxicity. Environmental Health Perspectives, **112**(14), 1347–1358. (2004).

19. Steiner, S., Bisig, C., Petri-Fink, A., & Rothen-Rutishauser, B. Diesel exhaust: current knowledge of adverse effects and underlying cellular mechanisms. Archives of Toxicology, **90**(7), 1541–1553. (2016).

20. Dellinger, B., D'Alessio, A., D'Anna, A., Ciajolo, A., Gullett, B., Henry, H., Keener, M., Lighty, J. A., Lomnicki, S., Lucas, D., Oberdörster, G., Pitea, D., Suk, W., Sarofim, A., Smith, K. R., Stoeger, T., Tolbert, P., Wyzga, R., Zimmermann, R. Combustion byproducts and their health effects: Summary of the 10th international congress. *Environmental Engineering Science*, **25**(8), 1107–1114. (2008).

21. Kwon, H. S., Ryu, M. H., Carlsten, C. Ultrafine particles: unique physicochemical properties relevant to health and disease. Experimental and Molecular Medicine, **52**(3), 318–328. (2020).

22. K. Lehtoranta, P. Aakko-Saksa, T. Murtonen, H. Vesala, L. Ntziachristos, T. Rönkkö, P. Karjalainen, N. Kuittinen, H. Timonen. *Environmental Science & Technology* **53**(6), 3315-3322 (2019).

23. J. Alanen, M. Isotalo, N. Kuittinen, P. Simonen, S. Martikainen, H. Kuuluvainen, M. Honkanen, K. Lehtoranta, S. Nyyssönen, H. Vesala, H. Timonen, M. Aurela, J. Keskinen, T. Rönkkö. *Environmental Science & Technology*, **54**(9), 5376-5384 (2020).

24. Lack, D. A., Corbett, J. J., Onasch, T., Lerner, B., Massoli, P., Quinn, P. K., Bates, T. S., Covert, D. S., Coffman, D., Sierau, B., Herndon, S., Allan, J., Baynard, T., Lovejoy, E., Ravishankara, A. R., Williams, E. Particulate emissions from commercial shipping: Chemical, physical, and optical properties. *J. Geophys. Res.* **114**(4), (2009).

25. J. M. Diesch, F. Drewnick, T. Klimach, S. Borrmann. Investigation of gaseous and particulate emissions from various marine vessel types measured on the banks of the Elbe in Northern Germany. *Atmos. Chem. Phys.* **13,** 3603–3618 (2013).

26. Å. M. Jonsson, J. Westerlund, M. Hallquist. Size-resolved particle emission factors for individual ships. *Geophys. Res. Lett.* **38,** 1–5 (2011).

27. Hobbs, P. V, Garrett, T. J., Ferek, R. J., Strader, S. R., Hegg, D. A., Frick, G. M., Hoppel, W. A., Gasparovic, R. F., Russell, L. M., Johnson, D. W., O'Dowd, C., Durkee, P. A., Nielsen, K. E., & Innis, G. Emissions from Ships with respect to Their Effects on Clouds. *J. Atmos. Sci.* **57,** 2570–2590 (2000).

28. Chen, G., Huey, L. G., Trainer, M., Nicks, D., Corbett, J., Ryerson, T., Parrish, D., Neuman, J. A., Nowak, J., Tanner, D., Holloway, J., Brock, C., Crawford, J., Olson, J. R., Sullivan, A., Weber, R., Schauffler, S., Donnelly, S., Atlas, E., Roberts, J., Flocke, F., Hübler, G., Fehsenfeld, F. An investigation of the chemistry of ship emission plumes during ITCT 2002. *J. Geophys. Res. D Atmos.* **110,** 1–15 (2005).

29. Petzold, A., Hasselbach, J., Lauer, P., Baumann, R., Franke, K., Gurk, C., Schlager, H., & Weingartner, E. Experimental studies on particle emissions from cruising ship, their characteristic properties, transformation and atmospheric lifetime in the marine boundary layer. *Atmos. Chem. Phys. Discuss.* **7**, 15105–15154 (2008).

30. Murphy, S., Agrawal, H., Sorooshian, A., Padr??, L. T., Gates, H., Hersey, S., Welch, W. A., Jung, H., Miller, J. W., Cocker, D. R., Nenes, A., Jonsson, H. H., Flagan, R. C., Seinfeld, J. H. Comprehensive simultaneous shipboard and airborne characterization of exhaust from a modern container ship at sea. *Environ. Sci. Technol.* **43**, 4626–4640 (2009).

31. Lack, D. A., Cappa, C. D., Langridge, J., Bahreini, R., Buffaloe, G., Brock, C., Cerully, K., Coffman, D., Hayden, K., Holloway, J., Lerner, B., Massoli, P., Li, S. M., McLaren, R., Middlebrook, A. M., Moore, R., Nenes, A., Nuaaman, I., Onasch, T. B., Peischl, J., Perring, A., Quinn, P., Ryerson, T., Schwartz, J. P., Spackman, R., Wofsy, S. C., Worsnop, D., Xiang, B., Williams, E. Impact of fuel quality regulation and speed reductions on shipping emissions: Implications for climate and air quality. *Environ. Sci. Technol.* **45,** 9052–9060 (2011).

32. Sinha, P., Hobbs, P. V., Yokelson, R. J., Christian, T. J., Kirchstetter, T. W., Bruintjes, R. Emissions of trace gases and particles from two ships in the southern Atlantic Ocean. *Atmos. Environ.* **37**, 2139–2148 (2003).

33. Cappa, C. D., Williams, E. J., Lack, D. a., Buffaloe, G. M., Coffman, D., Hayden, K. L., Herndon, S. C., Lerner, B. M., Li, S. M., Massoli, P., McLaren, R., Nuaaman, I., Onasch, T. B., Quinn, P. K. A case study into the measurement of ship emissions from plume intercepts of the NOAA ship Miller Freeman. *Atmos. Chem. Phys.* **14**, 1337–1352 (2014).

34. Aliabadi, A. A., Thomas, J. L., Herber, A. B., Staebler, R. M., Leaitch, W. R., Schulz, H., Law, K. S., Marelle, L., Burkart, J., Willis, M. D., Bozem, H., Hoor, P. M., Köllner, F., Schneider, J., Levasseur, M., Abbatt, J. P. D. Ship emissions measurement in the Arctic by plume intercepts of the Canadian Coast Guard icebreaker Amundsen from the Polar 6 aircraft platform. *Atmos. Chem. Phys.* **16**, 7899–7916 (2016).

35. L. Ntziachristos, Z. Samaras. The Potential of a Partial-Flow Constant Dilution Ratio Sampling System as a Candidate for Vehicle Exhaust Aerosol. *J. Air Waste Manage. Assoc.* **60**, 1223–1236 (2010).

36. B. Giechaskiel, L. Ntziachristos, Z. Samaras. Calibration and modelling of ejector dilutors for automotive exhaust sampling. *Meas. Sci. Technol.* **15**, 2199–2206 (2004).

37. Giechaskiel, B., Ntziachristos, L., Samaras, Z., Scheer, V., Casati, R., Vogt, R. Formation potential of vehicle exhaust nucleation mode particles on-road and in the laboratory. *Atmos. Environ.* **39**, 3191–3198 (2005).

38. J. Keskinen, T. Rönkkö. Can real-world diesel exhaust particle size distribution be reproduced in the laboratory? A critical review. J. Air *Waste Manag. Assoc.* **60**, 1245–1255 (2010).

39. Rönkkö, T., Virtanen, A., Vaaraslahti, K., Keskinen, J., Pirjola, L., Lappi, M. Effect of dilution conditions and driving parameters on nucleation mode particles in diesel exhaust: Laboratory and on-road study. *Atmos. Environ.* **40**, 2893–2901 (2006).

40. Chen, H., Winderlich, J., Gerbig, C., Hoefer, A., Rella, C. W., Crosson, E. R., Van Pelt, A. D., Steinbach, J., Kolle, O., Beck, V., Daube, B. C., Gottlieb, E. W., Chow, V. Y., Santoni, G. W., Wofsy, S. C. High-accuracy continuous airborne measurements of greenhouse gases (CO_2 and

CH₄) using the cavity ring-down spectroscopy (CRDS) technique. *Atmos. Meas. Tech.*, **3**, 375–386. (2010).

41. H. Tammet, A. Mirme, E. Tamm. Electrical aerosol spectrometer of Tartu University. *Atmos. Res.* **62**, 315–324 (2002).

42. Pirjola, L., Pajunoja, a., Walden, J., Jalkanen, J. P., Rönkkö, T., Kousa, A., Koskentalo, T. Mobile measurements of ship emissions in two harbour areas in Finland. *Atmos. Meas. Tech.* **7**, 149–161 (2014).

43. M. Righi, J. Hendricks, R. Sausen. The global impact of the transport sectors on atmospheric aerosol in 2030-Part 1: Land transport and shipping. *Atmos. Chem. Phys.* **15**, 633–651 (2015).

44. Jalkanen, J.-P. P., brink, A., Kalli, J., Pettersson, H., Kukkonen, J., Stipa, T. Modelling system for the exhaust emissions of marine traffic and its application in the Baltic Sea area. *Atmos. Chem. Phys.* **9**, 9209–9223 (2009).

45. Jalkanen, J., Johansson, L., Kukkonen, J., Brink, A., Kalli, J., Stipa, T. Extension of an assessment model of ship traffic exhaust emissions for particulate matter and carbon monoxide. *Atmos. Chem. Phys.* **12**, 2641–2659 (2012).

46. L. Johansson, J.-P. Jalkanen, J. Kalli, J. Kukkonen. The evolution of shipping emissions and the costs of regulation changes in the northern EU. *Atmos. Chem. Phys.* **13**, 11375–11389 (2013).

47. L. Johansson, J.-P. Jalkanen, J. Kukkonen. Global assessment of shipping emissions in 2015 on a high spatial and temporal resolution. *Atmos. Environ.* **167**, 403–415 (2017).

48. L. Johansson, E. Ytreberg, J.-P. Jalkanen, E. Fridell, K. M. Eriksson, M. Lagerström, I. Maljutenko, U. Raudsepp, V. Fischer, E. Roth. Model for leisure boat activities and emissions – implementation for the Baltic Sea. Ocean Science Discussions (2020, in review).

49. Faber, J., Ahdour, S., Hoen, M., Nelissen, D., Singh, A., Steiner, P., Rivera, S., Raucci, C., Smith, T., Muraoka, E., Ruderman, Y., Khomutov, I., Hanayama, S. "Assessment of fuel oil availability". (Publication 16.7G.68.71, CE Delft, 2016; https://cedelft.eu/publicatie/assessment_of_fuel_oil_availability/1858).

50. "Supplemental Marine Fuel Availability Study" (EnSys Energy and Navigistics Consulting, 2016); https://www.ensysenergy.com/downloads/supplemental-marine-fuels-availability-study-2/).

51. IMO MEPC70/18/Add.1, Annex 9, http://www.imo.org/en/KnowledgeCentre/IndexofIMOResolutions/Marine-Environment-Protection-Committee-%28MEPC%29/Documents/MEPC.281%2870%29.pdf

52. N. R. Gysel, W. A. Welch, K. Johnson, W. Miller, D. R. Cocker III. Detailed Analysis of Criteria and Particle Emissions from a Very Large Crude Carrier Using a Novel ECA Fuel. *Environ. Sci. Technol.* **51**, 1868–1875 (2017).

53. P. Aakko-Saksa, T. Murtonen, H. Vesala, P. Koponen, S. Nyyssönen, H. Puustinen, K. Lehtoranta, H. Timonen, K. Teinilä, R. Hillamo, P. Karjalainen, N. Kuittinen, P. Simonen, T. Rönkkö, J. Keskinen, E. Saukko, M. Tutuianu, R. Fischerleitner, L. Pirjola, O.-P. Brunila, E. Hämäläinen, E. Black Carbon measurements using different marine fuels. 28th CIMAC Congress, Helsinki, Finland (2016).

54. Kasper, A., Aufdenblatten, S., Forss, A., Mohr, M. & Burtscher, H. Particulate Emissions from a Low-Speed Marine Diesel Engine. *Aerosol Sci. Technol.* **41,** 24–32 (2007).

55. Zhou, S., Zhou, J., Zhu, Y. Chemical composition and size distribution of particulate matters from marine diesel engines with different fuel oils. *Fuel* **235,** 972–983 (2019).

56. E. Fridell, K. Salo. Measurements of abatement of particles and exhaust gases in a marine gas scrubber. *Eng. Marit. Environ.* **230**, 154–162 (2014).

57. Winnes, H., Fridell, E., Moldanová, J. (2020). Effects of marine exhaust gas scrubbers on gas and particle emissions. *Journal of Marine Science and Engineering*, **8**(4).

58. V. Eyring, H. W. Köhler, J. van Aardenne, A. Lauer. Emissions from international shipping: 1. The last 50 years. *J. Geophys. Res.* **110**, D17305 (2005).

59. C. Andersson, R. Bergström, C. Johansson. Population exposure and mortality due to regional background PM in Europe - Long-term simulations of source region and shipping contributions. *Atmos. Environ.* **43**, 3614–3620 (2009).

60. Paasonen, P., Kupiainen, K., Klimont, Z., Visshedijk, A., Denier van der Gon, H. A. C., Amann, M. Continental anthropogenic primary particle number emissions. *Atmos. Chem. Phys. Discuss,* **16**, 6823-6840. (2016).

61. Wu, D., Li, Q., Ding, X., Sun, J., Li, D., Fu, H., Teich, M., Ye, X., & Chen, J. Primary Particulate Matter Emitted from Heavy Fuel and Diesel Oil Combustion in a Typical Container Ship: Characteristics and Toxicity. *Environmental Science and Technology*, **52**(21), 12943–12951. (2018).

62. Ye, Q., Li, H. Z., Gu, P., Robinson, E. S., Apte, J. S., Sullivan, R. C., Robinson, A. L., Donahue, N. M., Presto, A. A. (2020). Moving beyond fine particle mass: High-spatial resolution exposure to source-resolved atmospheric particle number and chemical mixing state. *Environmental Health Perspectives*, **128**(1), 1–10.

63. Jones, R.R., Hoek, G., Fisher, J.A., Hasheminassab, S., Wang, D., Ward, M.H., Sioutas, C., Vermeulen, R., Silverman, D.T. (2020). Land use regression models for ultrafine particles, fine particles, and black carbon in Southern California. *Science of the Total Environment*, 699, Article number 134234.

64. Simon, M.C., Naumova, E.N., Levy, J.I., Brugge, D., Durant, J.L. (2020). Ultrafine Particle Number Concentration Model for Estimating Retrospective and Prospective Long-Term Ambient Exposures in Urban Neighborhoods. *Environmental Science and Technology*, **54**(3), 1677-1686

65. Saha, P.K., Sengupta, S., Adams, P., Robinson, A.L., Presto, A.A. (2020). Spatial Correlation of Ultrafine Particle Number and Fine Particle Mass at Urban Scales: Implications for Health Assessment. *Environmental Science and Technology*. **54**(15), 9295-9304

66. Xausa, F., Paasonen, P., Makkonen, R., Arshinov, M., Ding, A., Denier Van Der Gon, H., Kerminen, V. M., & Kulmala, M. (2018). Advancing global aerosol simulations with size-segregated anthropogenic particle number emissions. *Atmospheric Chemistry and Physics,* **18**(13), 10039–10054.

62. Alföldy, B., Lööv, J. B., Lagler, F., Mellqvist, J., Berg, N., Beecken, J., Weststrate, H., Duyzer, J., Bencs, L., Horemans, B., Cavalli, F., Putaud, J. P., Janssens-Maenhout, G., Csordás, A. P., Van Grieken, R., Borowiak, A., & Hjorth, J. Measurements of air pollution emission factors for marine transportation in SECA. *Atmos. Meas. Tech.* **6,** 1777–1791 (2013).